Received: 5 May 2022 | Revised: 3 August 2022 | Accepted: 30 August 2022

DOI: 10.1111/aor.14405

Artificial Organs WILEY

MAIN TEXT

Comparison of hemodynamics in biological surgical aortic valve replacement and transcatheter aortic valve implantation: An in-silico study

Benedikt Franke[1] | **Adriano Schlief**[1] | **Lars Walczak**[1,2] | **Simon Sündermann**[3,4] | **Axel Unbehaun**[4,5] | **Jörg Kempfert**[4] | **Natalia Solowjowa**[4] | **Titus Kühne**[1,5] | **Leonid Goubergrits**[1,6]

[1]Institute of Computer-assisted Cardiovascular Medicine, Charité—Universitätsmedizin Berlin, Berlin, Germany

[2]Fraunhofer MEVIS, Bremen, Germany

[3]Department of Cardiology and Angiology, Charité—Universitätsmedizin Berlin, Berlin, Germany

[4]Department of Cardiothoracic and Vascular Surgery, German Heart Center Berlin, Berlin, Germany

[5]DZHK (German Centre for Cardiovascular Research), Partner Site Berlin, Berlin, Germany

[6]Einstein Center Digital Future, Berlin, Germany

Correspondence
Benedikt Franke, Charité—Universitätsmedizin Berlin, Institute of Computer-assisted Cardiovascular Medicine, Berlin, Germany.
Email: benedikt.franke@charite.de

Abstract

Objectives: In aortic valve replacement (AVR), the treatment strategy as well as the model and size of the implanted prosthesis have a major impact on the postoperative hemodynamics and thus on the clinical outcome. Preinterventional prediction of the hemodynamics could support the treatment decision. Therefore, we performed paired virtual treatment with transcatheter AVR (TAVI) and biological surgical AVR (SAVR) and compared hemodynamic outcomes using numerical simulations.

Methods: 10 patients with severe aortic stenosis (AS) undergoing TAVI were virtually treated with both biological SAVR and TAVI to compare post-interventional hemodynamics using numerical simulations of peak-systolic flow. Virtual treatment procedure was done using an in-house developed tool based on position-based dynamics methodology, which was applied to the patient's anatomy including LVOT, aortic root and aorta. Geometries were automatically segmented from dynamic CT-scans and patient-specific flow rates were calculated by volumetric analysis of the left ventricle. Hemodynamics were assessed using the STAR CCM+ software by solving the RANS equations.

Results: Virtual treatment with TAVI resulted in realistic hemodynamics comparable to echocardiographic measurements (median difference in transvalvular pressure gradient [TPG]: −0.33 mm Hg). Virtual TAVI and SAVR showed similar hemodynamic functions with a mean TPG with standard deviation of 8.45 ± 4.60 mm Hg in TAVI and 6.66 ± 3.79 mm Hg in SAVR ($p = 0.03$) while max. Wall shear stress being 12.6 ± 4.59 vs. 10.2 ± 4.42 Pa ($p = 0.001$).

Conclusions: Using the presented method for virtual treatment of AS, we were able to reliably predict post-interventional hemodynamics. TAVI and SAVR show similar hemodynamics in a pairwise comparison.

KEYWORDS

hemodynamics, surgical aortic valve replacement, TAVI, virtual treatment

1 | BACKGROUND

In developed countries, aortic stenosis (AS) is the third most frequent cardiovascular disease, with only coronary artery disease and systemic arterial hypertension being more common.[1] While being low in the young population, prevalence rises with age, resulting in 1 in 8 people being affected at the age of 75 or older.[2] AS can remain asymptomatic for years and at this stage has a relatively low risk of sudden death of approximately 1% per year.[3,4] However, when symptoms occur, the risk increases abruptly, resulting in three-quarters of patients dying within 3 years if untreated.[5] For symptomatic, hemodynamically severe AS, aortic valve replacement (AVR) is the only effective treatment.

AVR can be performed using two techniques: Surgical aortic valve replacement (SAVR) in which the aortic valve (AV) is replaced by a mechanical or biological valve prosthesis or transcatheter aortic valve implantation (TAVI) in which a biological valve prosthesis mounted on a stent is implanted via minimal invasive catheter. The decision as to which procedure to use must be weighed individually and depends on many factors, such as surgical risk, the need for anticoagulation, or the patient's age and personal preference. While SAVR has been the standard procedure for symptomatic severe AS for 50 years, TAVI was established in the last 10 years as an alternative procedure for patients with high or prohibitive operative risk. The reason for TAVI's limitation in use mainly lies in the lack of data on its long-term reliability. In recent years, however, a trend toward TAVI has been observed. In the United States, about 30% of all AVR are already performed via TAVI-technique, while in Germany TAVI has overtaken SAVR as the definitive treatment for AS (2 out of 3 treatments).[6,7] In terms of hemodynamic function like transvalvular pressure gradient (TPG) or paravalvular leakage ambiguous results have been published, with some studies reporting SAVR to be superior in terms of hemodynamics and others favoring TAVI.[8–11]

For further studies in this field, an age-matched comparative study would be ideal from a statistical point of view but does not seem to be reasonable from a clinical point of view, as patient cohorts mostly differ due to the differences in each procedure's inclusion criteria, leading to an unequal baseline regarding anatomy and physiology.[12] Therefore, our goal was to pairwise compare hemodynamics of patients, virtually treated with both procedures—TAVI and SAVR. For this, the patient's anatomy was segmented from computed tomography (CT) image data and virtual aortic valve replacement was performed using an in-house developed tool. Finally, patient-specific hemodynamics were calculated numerically and compared for each valve in a paired analysis.

2 | METHODS

2.1 | Cohort description

The dataset used in this study was obtained from a retrospective study published earlier.[13] Briefly, these are patients suffering from severe aortic valve stenosis who underwent TAVI-procedure at the German Heart Center Berlin between February and April 2019. The dataset contains spatially and temporally highly resolved Computed Tomography (CT) images and post-interventional measurements of the trans-valvular blood velocity done via Doppler echocardiography from 10 patients (9 female). The patients' baseline characteristics are shown in Table 1.

The study was registered at ClinicalTrials.gov (NCT04600739) and was approved by the internal review board (EA2/174/19). Individual informed consent was waived by the IRB due to the retrospective nature of this study.

2.2 | Data preparation

For each case, the anatomy of the left ventricle, AV and aorta during the end-systolic phase was reconstructed from CT-data using an approach described earlier.[14] The reconstructed geometry was smoothed and checked for intersections, manifolds and holes using Meshmixer (v. 11.0.544, Autodesk, California, USA). Further, the left ventricle was cut at the level of the left ventricular outflow tract and the AV leaflets were removed for virtual valve replacement as described later.

To evaluate hemodynamics after virtual valve replacement, numerical simulations were performed using patient-specific flow rates.

TABLE 1 Patient's baseline characteristics

Parameter	Median [25th–75th percentile]
Female sex, *n* (%)	9 (90)
Age [years]	82 [79–87]
Body surface area [m^2]	1.58 [1.48–1.77]
Heart rate [bpm]	71 [64–81]
Transvalvular v_{max} [m/s]	4.1 [3.5–4.6]
Echo-measured mean transvalvular pressure gradient [mm Hg]	47 [31–50]
Catheter-measured peak systolic pressure gradient [mm Hg]	57 [41–71]
Aortic valve insufficiency, *n* (%)	5 (50)
Mitral valve insufficiency, *n* (%)	9 (90)
Left ventricular ejection fraction (%)	60 [60–67]

For this, the volumetric change in the LV during the systolic phase was calculated by segmenting the LV for each phase and calculating the differences in volume between phases. The change in volume was then divided by the time step between two subsequent phases and the highest value representing peak systolic flow was chosen. In case of a concomitant mitral valve insufficiency (MI), regurgitation was considered by reducing aortic flow by 10%, 30% and 50% for mild, moderate, and severe MI. The narrowest area of the virtual implanted protheses in fully opened stage determined the geometric orifice area (GOA).

For each geometry, a centerline was created using ZIBAmira (v. 2015.28, Zuse Institute Berlin, Berlin, Germany). The centerline was required for the placement of the prothesis within the aortic root during virtual AVR as well as for analysis of the hemodynamics (static pressure and wall shear stress).

2.3 | Virtual aortic valve replacement

For virtual AVR, geometric representations of TAVI and SAVR protheses were generated. For TAVI, models of the real procedures were used while for SAVR the Carpentier-Edwards Magna Ease prosthesis was used (see Figure 1). Prosthesis size was determined by a cardiac surgeon after analyzing the CT-data using 3mensio (Pie Medical Imaging BV, Maastricht, the Netherlands) in the following way: Annulus dimensions were assessed by marking the three nadirs of the aortic valve and measuring the resulting area. The area-derived diameter was used to estimate the prothesis size. Additionally, anatomical features like calcifications or ovality of the anulus were considered as well as surgical specifics like the supra-annular placement of the prosthesis. For the reconstruction of the prostheses, a micro-scan of the SAPIEN 3 prothesis size 23 and 29 in open position was done using a multi-slice spiral CT scanner (Somatom Definition Flash, Siemens Healthineers, Erlangen, Germany). The spatial resolution used for reconstruction was 0.252 mm × 0.252 mm in-plane resolution and 0.75 mm slice thickness. The valve's geometry was reconstructed from the CT-data using ZIBAmira. Since only one SAPIEN 3 prosthesis was available as a model for reconstruction, the other prostheses and sizes used in the intervention were estimated by scaling the SAPIEN's geometry according to the dimensions given by the manufacturers. Representations of the Carpentier-Edwards Magna Ease (Figure 1) were generated as described in Hellmeier et al.[15] For virtual AVR-procedure, two free edge loops were added to the annular base of the valve, projecting above and below the valve as cylinder-shaped extensions, enabling a merging to the aorta's geometry and achieving the correct mesh topology.

To generate geometries for the flow simulation we used the approach presented by Walczak et al.[16] As input, triangle meshes of the aorta and the valve model, as well as the aorta's centerline, were required. The valve model was placed along the centerline and transformed from its local coordinate system to the local TNB frame (tangent, normal, binormal) of the centerline to achieve an initial orientation in world coordinates. Movements in the plane originating at the centerline position, spanned by normal and binormal were available as well as rotations around the TNB axis to place the valve prosthesis model in the aortic root.

After placement of the valve, merging was achieved as follows (Figure 2): Rays originating from the valve's edge vertices were cast radially outwards till intersecting with

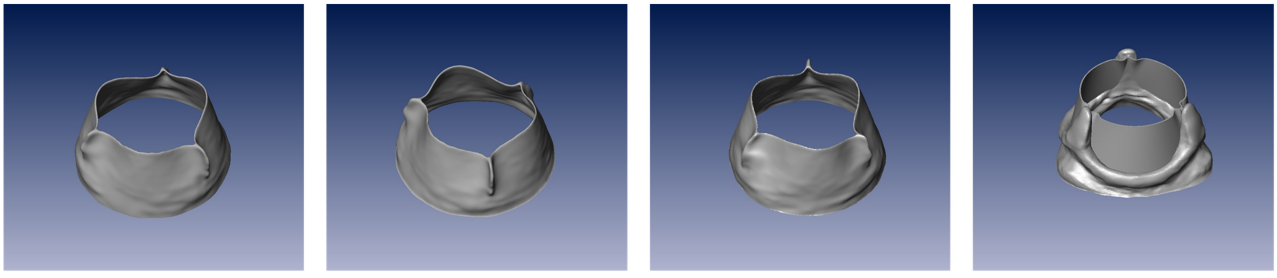

Case-ID	1	2	3	4	5	6	7	8	9	10
TAVI	Evolut PRO 26	Evolut PRO 26	SAPIEN 3 23	Evolut PRO 29	SAPIEN 3 26	Evolut PRO 26	Evolut R 26	Evolut PRO 26	Evolut PRO 26	ALLEGRA 23
SAVR*	21 mm	23 mm	21 mm	23 mm	25 mm	19 mm	21 mm	23 mm	21 mm	19 mm

* Carpentier-Edwards Magna Ease was used for all cases

FIGURE 1 Models and sizes of AVR used in this study. From left to right: Edwards Sapien S3 (Edwards Lifesciences, California, U.S), Medtronic CoreValve Evolut PRO / R (Medtronic plc, Dublin, Ireland), new valve technology Allegra (NVT AG, Morges, Switzerland), Carpentier-Edwards magna ease (Edwards Lifesciences, California, USA).

the aortic mesh. For 1-to-1 mapping of the edge loop's vertices and their projections on the aorta, the paths between vertices were post-processed using edge flipping and edge contraction and elements on a path between two projected points were removed. Afterwards, mesh elements between both projected edge loops were removed, bisecting the aortic mesh into a part anterior and a part posterior to the valve's loop. To merge the vertices of the edge loops and the projections, the aorta was modeled as a soft body with elastic properties, whereas the rays cast were modeled as contracting springs with a rest length of zero. In addition, a pressure force was applied to deform the aortic mesh in a user-defined region. Once the projected vertices were converged to their target position of the valve edge loop vertices, deformation stopped, and both meshes were merged into one. The resulting mesh is topologically consistent and exhibits a smooth transition from the ring-shaped base of the valve to the aorta. In the following, virtually implanted TAVI cases will be abbreviated as $TAVI_{virt}$ and SAVR as $SAVR_{virt}$, respectively.

2.4 | Numerical simulation

Numerical calculations of patient-specific hemodynamics were performed using Simcenter STAR-CCM+ (v. 15.02.007, Siemens PLM Software Inc., Texas, USA), which uses a finite volume discretization to solve the Navier–Stokes equations. Polyhedral volume meshes were created using the integrated meshing algorithm as described earlier[14]: For all cases a base size of 0.4 mm was set, as found to be sufficient in the mesh-independence study (Figure S1). The boundary regions of the aorta wall and the prosthesis were refined using a prism layer consisting of 7 cells (initial thickness: 0.13 mm, 20% increase for each layer) to correctly calculate near-wall flow and wall-shear stress. The resulting meshes had a cell count of 3 to 5 Mio cells and was of good quality according to the mesh-quality metrics: cell quality, cell aspect ratio, skewness angle and volume change (Table S1).

At the inlet, the patient-specific peak-systolic mass flow rate based on CT-data was applied. Vessel walls were defined as rigid with a no-slip condition. The end of the descending aorta was defined as a flow split outlet boundary. An implicit steady-state solver was used. Density of blood was set to $\rho = 1050\,kg/m^3$. Dynamic viscosity was modeled using the generalized Carreau-Yasuda model with parameters for blood proposed by Abraham et al.[17] The threshold kinematic viscosity of the viscosity model was set to $\eta = 0.0035$ Pa s. Turbulence was modeled using the shear-stress transport (SST) k-omega solver.

To evaluate the hemodynamic function, we analyzed the numerically calculated max. TPG and max. Wall shear stress (WSS) at peak-systolic flow. For TPG, cross-sectional averaged pressure was measured upstream of the valve within the smallest diameter in the region between LVOT and AV as well as in the ascending aorta, at the position where the pressure recovery was maximal due to the deceleration of blood. Max. TPG was calculated as the difference of both values. For analysis of the wall shear stress both the maximum value of the surface averaged WSS and its position were examined.

2.5 | Statistics

Differences between the prosthesis geometric valve area, max. TPG, and max. WSS were tested for significance. Here, the differences were tested for normal distribution using the Shapiro–Wilk test. Normally distributed data was represented as mean with standard deviation, otherwise as median and interquartile range [IQR]. In case of normal distribution, a paired-samples *t*-test was used. Otherwise, differences were tested using a Wilcoxon signed-rank test. All tests were done using SPSS Statistics (v. 25, IBM, Armonk, New York, USA).

Measurement of the GOA revealed a significantly smaller orifice area in $TAVI_{virt}$ than in $SAVR_{virt}$ (median and interquartile range (IQR) of 1.85 [0.21] cm^2 vs. 2.25 [0.57]cm^2,

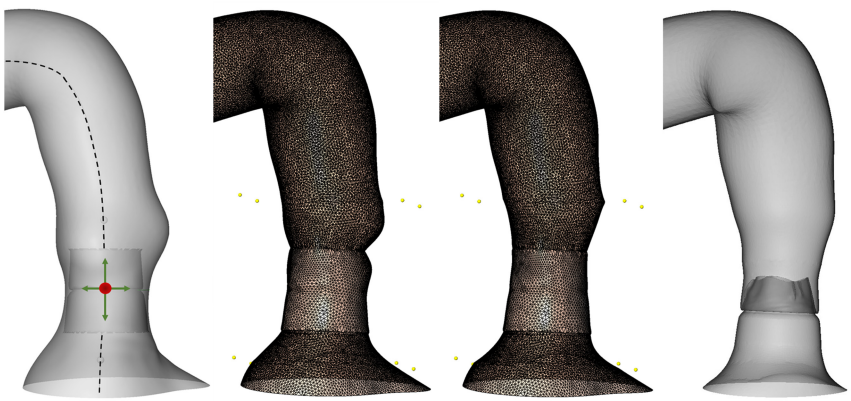

FIGURE 2 Virtual aortic valve replacement. Positioning of the valve model within the aortic root (left). Merging process of valve and aorta (middle). Final geometry used for numerical simulation (right).

$p = 0.005$). This contrasts with findings of Pibarot et al stating that in patients with comparable anulus diameter, the orifice area of TAVI and SAVR does not differ.[8] Since selection of SAVR size based on MDCT usually results in an oversizing of at least one size,[15,18] we decided to virtually implant each patient with a SAVR prosthesis one size smaller than the one originally selected, except for cases 7 and 15, since the narrowest prosthesis was already selected here.

3 | RESULTS

Using the method described above, we were able to merge prosthesis and aorta representation successfully and perform numerical calculations. The median of GOA was 1.85 [0.21] cm^2 in $TAVI_{virt}$ and 1.87 [0.38] cm^2 in $SAVR_{virt}$ while being comparable ($p = 0.501$). Mean and standard deviation of patient-specific flow rate was 251.5 ± 74.35 ml/s.

To verify simulations, we compared post-interventional TPG in $TAVI_{virt}$ with clinical echocardiographic TPG_{max} measured within 3 days after intervention. As shown in Figure 3 simulated $TAVI_{virt}$ showed good agreement with real TAVI regarding TPG. The median difference between echocardiographic measured TPG and simulated TPG was 0.33 mm Hg. Only in one case a difference higher than 10 mm Hg between $TAVI_{virt}$ and real TAVI was observed. Patient 3 died shortly after the intervention before hemodynamics were evaluated. Overall virtual treatment resulted in a significantly reduced TPG compared to pre-interventional measurements (paired *t*-test: $p = 0.001$). Echocardiographic TPG_{max} decreased from 67.1 ± 24.20 mm Hg to 8.45 ± 4.60 mm Hg in simulated $TAVI_{virt}$. TPG was comparable to TAVI in $SAVR_{virt}$ with a TPG of 6.66 ± 3.79 mm Hg ($p = 0.03$), as can be seen in Table 2.

Simulated max. WSS was 12.58 ± 4.59 Pa vs. 10.22 ± 4.42 Pa for $TAVI_{virt}$ and $SAVR_{virt}$ (paired *t*-test: $p = 0.001$). The distance of the position of highest WSS to the anulus plane did not differ substantially between the procedures being between 51 mm and 74 mm posterior to the valve. As shown in Figure 4, the jet passing through the aortic valve was mostly slightly narrower in $TAVI_{virt}$ and in average had a higher velocity compared to $SAVR_{virt}$. In some $SAVR_{virt}$ cases vortices can be observed anterior to the valve, indicating a suboptimal transition from aorta to prosthesis.

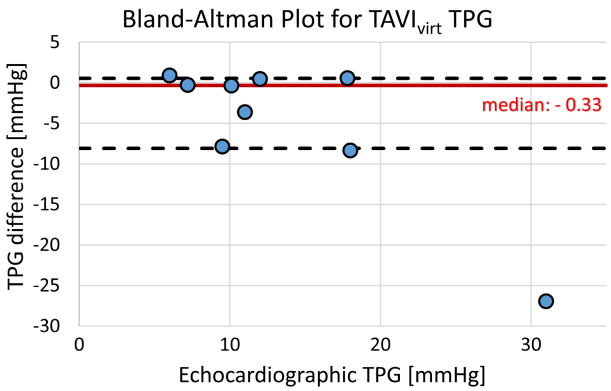

FIGURE 3 Differences in TPG between $TAVI_{virt}$ and real TAVI

4 | DISCUSSION

Using the described approach for virtual treatment of AVR-patients, we were able to simulate post-interventional hemodynamics and compare the hemodynamic functions of TAVI and SAVR in a pairwise manner. The virtual treatment led to promising results, significantly reducing TPG compared to pre-interventional data. Post-interventional TPG agreed well between $TAVI_{virt}$ and real TAVI with the difference between both procedures being less than 10 mm Hg in all cases, except for case 1. In this patient, a

TABLE 2 Post-procedural hemodynamics in $TAVI_{virt}$ and $SAVR_{virt}$

Case ID	Echocardiographic TPG_{max}, mm Hg	$TAVI_{virt}$ TPG, mm Hg	$SAVR_{virt}$ TPG, mm Hg	$TAVI_{virt}$ max. WSS, pa	$SAVR_{virt}$ max. WSS, pa
1	31	4.09	3.93	8.63	7.50
2	11	7.39	4.30	10.94	7.0
3	–	7.2	7.83	14.77	9.61
4	6	6.91	5.32	10.55	9.34
5	12	12.5	6.75	15.57	11.93
6	18	9.67	8.76	14.39	12.78
7	9.5	1.66	1.45	4.28	3.57
8	10.1	9.77	5.22	12.57	8.61
9	17.8	18.38	15.53	21.6	20.12
10	7.2	6.94	7.52	12.46	11.74

Abbreviations: TPG, transvalvular pressure gradient; WSS, wall shear stress.

FIGURE 4 Patient-specific hemodynamics visualized using streamlines. Cases virtually treated with TAVI (right) show slightly higher velocities than cases virtually treated with SAVR (left).

relatively high postinterventional TPG of 31 mm Hg was observed, suggesting errors during the echocardiographic procedure or challenges during the intervention which were not reflected in the virtual treatment and therefore possibly explaining the high differences in TPG.

Unfortunately, no post-interventional measurements on the TAVI's EOA were available. Therefore, an additional verification of $TAVI_{virt}$ based on the orifice area was not possible. However, there are several studies that have focused on TAVI's performance including EOA. Hahn et al e.g., evaluated hemodynamics of different TAVI models based on data from thousands of patients.[10] Compared to this data the orifice area from our study is exclusively higher in all models ($1.45 \pm 0.26\,cm^2$ vs. $1.97\,cm^2$ and $1.74 \pm 0.35\,cm^2$ vs. $2.45\,cm^2$ for the Sapien and $1.69 \pm 0.40\,cm^2$ vs. $1.85\,cm^2$ and $1.97 \pm 0.54\,cm^2$ vs. $2.34\,cm^2$ for the Evolut Pro). However, it is important to note that Hahn et al referred to the effective orifice area which is known to be significantly larger than the geometric orifice area, used in our study.[19,20] Nevertheless, risk remains that the forced, complete opening of the prosthesis during virtual treatment was not done to this extent in the real procedure and $TAVI_{virt}$ therefore displays an idealized hemodynamics.

Hemodynamics highly affect the treatment outcome of AVR-patients and are used as a marker for the intervention's success.[21–23] In addition to paravalvular leak, TPG is the main parameter to judge the success of the procedure and to estimate the patient's outcome.[21,22] Further, high WSS is known to promote the formation of aortic dilatation and aneurysms.[24] It is recommended to perform echocardiography before discharge or within 30 days after valve implantation as well as 1 year after valve implantation to evaluate for hemodynamic function.[25] Knowledge of prothesis-depending post-treatment hemodynamics could support treatment decisions by providing information about valve function before surgery, potentially preventing reinvention. There are several studies showing that hemodynamics differs between patients receiving SAVR and patients receiving TAVI.[8,9,11] A direct comparison of the hemodynamic function of the prostheses, however, appears to be of limited value, since patient cohorts differ based on (previous) clinical guidelines that recommend TAVI only for high-risk patients who are older and more fragile by nature. These patients tend to have a lower cardiac outcome and therefore a lower trans-valvular velocity and lower TPG. But there is a trend toward the use of TAVI in younger and healthier patients as more results about long-term reliability of TAVI are gained and guidelines are adjusted. For example, the recently published PARTNER 3 Trial demonstrated equivalence of TAVI over SAVR in patients at low and intermediate surgical risk regarding serious adverse events within 2 years after intervention, suggesting the suitability of TAVI also for this cohort.[26] Therefore, an increased overlap of patient populations is to be expected, which motivated our study. Our findings show, that SAVR results in comparable values for TPG and max. WSS when directly compared against TAVI. Unfortunately, no data about echocardiography measured EOA was available for the patients. Therefore, no further validation based on the orifice area was possible.

A known challenge associated with AVR is patient-prothesis-mismatch (PPM), meaning that the replaced valve is too small for the patient. Classification of PPM is based on the indexed effective orifice area, which is defined as the effective orifice area of the prosthesis normalized to the body surface. A meta-analysis of 34 studies showed that PPM was present in 44% of all patients who underwent AVR, of which 9.8% were severe, making it a widespread issue.[27] PPM is associated with structural valve degeneration and an increase in all-cause and cardiac-related mortality.[27,28] If a potential risk for PPM is identified during AVR planning, it can be prevented according to Pibarot by (1) choosing a newer generation of prosthetic with improved hemodynamic; (2) enlarging the aortic root or annulus to allow a larger prosthetic valve to fit; or (3) performing TAVI rather than SAVR as PPM is more common in surgical AVR.[29] Our results are partly in contrast to this recommendation since choosing TAVI over biological SAVR would not improve hemodynamics. Further studies need to be done on a larger number of patients with a comparable baseline between TAVI and SAVR patients. However, there are scenarios where our results may already help in the decision-making process. For example, in patients at risk of PPM in whom a normal TAVI procedure is not feasible, e.g., because of severe atherosclerosis, our results could favor SAVR in combination with a root dilation over transapical TAVI.

4.1 | Limitations

In this study, we analyzed a small cohort of 10 patients, 9 of whom were women. With a median age of 82 years and median weight of 54.5 kilograms patients were rather old and frail not representing the whole range of AS patients. Therefore, it stays uncertain whether these preliminary results can be generalized to all patients suffering from AS. The geometric representations of the patient's aorta and LVOT were done semi-automatically leaving the risk of not being accurate enough. However, since the same geometries were used for $TAVI_{virt}$ and $SAVR_{virt}$, the resulting error should be negligible.

Paravalvular leak (PVL), which is known to be more frequent in TAVI than in SAVR and is associated with poor outcome[23] was not analyzed in this study, since PVL does not affect the investigated parameters. However, considering the function of a prothesis, PVL is rightfully important and should be further investigated in future.

Pre-interventional sizing of SAVR remains challenging since there are several aspects that can only be assessed during treatment, like, e.g., decalcification. Basman et al, however, were able to correctly predict the SAVR size in AS patients in 94% of cases using preoperative MSCT only.[30] Whether the results of this small study are generally valid should be verified in a larger study.

5 | CONCLUSION

The study showed good results for virtual AVR with comparable values for TAVI and SAVR in terms of TPG and max. WSS. Whether these results can be generalized to all patients suffering from AS remains uncertain for now. It is planned to conduct a larger, prospective study with a more heterogeneous cohort in which virtual SAVR will be validated against real SAVR and EOA will be used as an additional validation parameter.

AUTHOR CONTRIBUTIONS

Concept/design: Benedikt Franke and Leonid Goubergrits. *Data analysis/interpretation*: Benedikt Franke and Leonid Goubergrits. *Drafting article*: Benedikt Franke, Leonid Goubergrits, Lars Walczak, and Simon Sündermann. *Methodology*: Benedikt Franke, Adriano Schlief, and Simon Sündermann. *Data collection*: Jörg Kempfert, Natalja Solowjowa, and Axel Unbehaun. *Funding secured by*: Titus Kühne and Leonid Goubergrits. *Critical revision of article*: Axel Unbehaun and Simon Sündermann. *Software*: Lars Walczak.

ACKNOWLEDGMENT

Open Access funding enabled and organized by Projekt DEAL.

CONFLICTS OF INTEREST

None declared.

ORCID

Benedikt Franke https://orcid.org/0000-0001-8742-3150
Leonid Goubergrits https://orcid.org/0000-0002-1961-3179

REFERENCES

1. Pibarot P, Dumesnil JG. New concepts in valvular hemodynamics: implications for diagnosis and treatment of aortic stenosis. Can J Cardiol. 2007 Oct;23(Suppl B):40B–7B.
2. Osnabrugge R, Mylotte D, Head S, Van Mieghem N, Nkomo V, LeReun C, et al. Aortic stenosis in the elderly: disease prevalence and number of candidates for transcatheter aortic valve replacement: a meta-analysis and modeling study. J Am Coll Cardiol. 2013;62(11):1002–12.
3. Rosenhek R, Binder T, Porenta G, Lang I, Christ G, Schemper M, et al. Predictors of outcome in severe, asymptomatic aortic stenosis. N Engl J Med. 2000 Aug 31;343(9):611–7.
4. Pellikka P, Sarano M, Nishimura R, Malouf J, Bailey K, Scott C, et al. Outcome of 622 adults with asymptomatic, hemodynamically significant aortic stenosis during prolonged follow-up. Circulation. 2005 Jun 21;111(24):3290–5.
5. Carabello B. Evaluation and management of patients with aortic stenosis. Circulation. 2002 Apr 16;105(15):1746–50.
6. Beckmann A, Meyer R, Lewandowski J, Markewitz A, Gummert J. German heart surgery report 2020: the annual updated registry of the German society for thoracic and cardiovascular surgery. Thorac Cardiovasc Surg. 2021 Jun;69(4):294–307.
7. Grover F, Vemulapalli S, Carroll J, Edwards F, Mack M, Thourani V, et al. 2016 annual report of the Society of Thoracic Surgeons/American College of Cardiology Transcatheter Valve Therapy Registry. J Am Coll Cardiol. 2017 Mar 14;69(10):1215–30.
8. Pibarot P, Salaun E, Dahou A, Avenatti E, Guzzetti E, Annabi MS, et al. Echocardiographic results of transcatheter versus surgical aortic valve replacement in low-risk patients: the PARTNER 3 trial. Circulation. 2020 May 12;141(19):1527–37.
9. Eghbalzadeh K, Rahmanian PB, Giese D, Kuhn EW, Djordjevic I, Kaya S, et al. SAVR versus TAVI: what about the hemodynamic performance? An in vivo and in vitro analysis. Thorac Cardiovasc Surg. 2020 Oct;68(7):608–15.
10. Hahn R, Pibarot P, Stewart W, Weissman N, Gopalakrishnan D, Keane M, et al. Comparison of transcatheter and surgical aortic valve replacement in severe aortic stenosis: a longitudinal study of echocardiography parameters in cohort a of the PARTNER trial (placement of aortic transcatheter valves). J Am Coll Cardiol. 2013 Jun 25;61(25):2514–21.
11. Little S, Oh J, Gillam L, Sengupta P, Orsinelli D, Cavalcante J, et al. Expanding transcatheter aortic valve replacement versus surgical valve replacement in patients at high risk for surgery: a study of echocardiographic change and risk prediction. Circ Cardiovasc Interv. 2016 Jun;9(6):e003426.
12. Ziv-Baran T, Zelman RB, Dombrowski P, Schaub AE, Mohr R, Loberman D. Surgical versus trans-catheter aortic valve replacement (SAVR vs TAVI) in patients with aortic stenosis: experience in a community hospital. Medicine (Baltimore). 2019 Nov;98(45):e17915.
13. Franke B, Brüning J, Yevtushenko P, Dreger H, Brand A, Juri B, et al. Computed tomography-based assessment of transvalvular pressure gradient in aortic stenosis. Front Cardiovasc Med. 2021;8:706628.
14. Franke B, Weese J, Waechter-Stehle I, Brüning J, Kuehne T, Goubergrits L. Towards improving the accuracy of aortic transvalvular pressure gradients: rethinking Bernoulli. Med Biol Eng Comput. 2020 Aug;58(8):1667–79.
15. Hellmeier F, Brüning J, Sündermann S, Jarmatz L, Schafstedde M, Goubergrits L, et al. Hemodynamic modeling of biological aortic valve replacement using preoperative data only. Front Cardiovasc Med. 2021 Feb;9(7):593709.
16. Walczak L, Goubergrits L, Hüllebrand M, Georgii J, Falk V, Hennemuth A. Using position-based dynamics to simulate deformation in aortic valve replacement procedure. Curr Dir Biomed Eng. 2020;6(1):20200042.
17. Abraham F, Behr M, Heinkenschloss M. Shape optimization in steady blood flow: a numerical study of non-Newtonian effects. Comput Methods Biomech Biomed Engin. 2005 Apr;8(2):127–37.
18. George I, Guglielmetti LC, Bettinger N, Moss A, Wang C, Kheysin N, et al. Aortic valve annular sizing: intraoperative assessment versus preoperative multidetector computed tomography. Circ Cardiovasc Imaging. 2017 May;10(5):e005968.
19. Habis M, Daoud B, Roger VL, Ghostine S, Caussin C, Ramadan R, et al. Comparison of 64-slice computed tomography planimetry and doppler echocardiography in the assessment of aortic valve stenosis. J Heart Valve Dis. 2007 May;16(3):216–24.
20. Adda J, Stanova V, Habib G, Rieu R. In vitro correlation between the effective and geometric orifice area in aortic stenosis. J Cardiol. 2021;77(4):334–40.
21. Dekany G, Fontos G, Satish S, Szabo G, Pinter T, Piroth Z, et al. The prognostic value of immediate post-TAVI hemodynamic evaluation is superior to aortography and transoesophageal echocardiography in predicting patient survival. Int J Cardiol. 2021 Apr;15(329):153–61.
22. Didier R, Benic C, Nasr B, Le Ven F, Hannachi S, Eltchaninoff H, et al. High post-procedural transvalvular gradient or delayed mean gradient increase after transcatheter aortic valve implantation: incidence, prognosis and associated variables. The France-2 registry. J Clin Med. 2021 Jul 22;10(15):3221.

23. Abdel-Wahab M, Zahn R, Horack M, Gerckens U, Schuler G, Sievert H, et al. Aortic regurgitation after transcatheter aortic valve implantation: incidence and early outcome. Results from the German transcatheter aortic valve interventions registry. Heart. 2011 Jun;97(11):899–906.
24. Staarmann B, Smith M, Prestigiacomo CJ. Shear stress and aneurysms: a review. Neurosurg Focus. 2019 Jul 1;47(1):E2.
25. Capodanno D, Petronio AS, Prendergast B, Eltchaninoff H, Vahanian A, Modine T, et al. Standardized definitions of structural deterioration and valve failure in assessing long-term durability of transcatheter and surgical aortic bioprosthetic valves: a consensus statement from the European Association of Percutaneous Cardiovascular Interventions (EAPCI) endorsed by the European Society of Cardiology (ESC) and the European Association for Cardio-Thoracic Surgery (EACTS). Eur Heart J. 2017 Dec 1;38(45):3382–90.
26. Leon M, Mack M, Hahn R, Thourani V, Makkar R, Kodali S, et al. Outcomes 2 years after transcatheter aortic valve replacement in patients at low surgical risk. J Am Coll Cardiol. 2021 Mar 9;77(9):1149–61.
27. Head S, Mokhles M, Osnabrugge R, Pibarot P, Mack M, Takkenberg J, et al. The impact of prosthesis-patient mismatch on long-term survival after aortic valve replacement: a systematic review and meta-analysis of 34 observational studies comprising 27 186 patients with 133 141 patient-years. Eur Heart J. 2012 Jun;33(12):1518–29.
28. Flameng W, Herregods MC, Vercalsteren M, Herijgers P, Bogaerts K, Meuris B. Prosthesis-patient mismatch predicts structural valve degeneration in bioprosthetic heart valves. Circulation. 2010 May 18;121(19):2123–9.
29. Pibarot P, Magne J, Leipsic J, Côté N, Blanke P, Thourani V, et al. Imaging for predicting and assessing prosthesis-patient mismatch after aortic valve replacement. JACC Cardiovasc Imaging. 2019 Jan;12(1):149–62.
30. Basman C, Seetharam K, Johnson J, Hemli JM, Brinster DR, Patel NC, et al. Preoperative multidetector computed tomography for isolated surgical aortic valve replacement: planning for future transcatheter options. J Card Surg. 2020 Dec;35(12):3354–3361.https://doi.org/10.1111/jocs.15080.

SUPPORTING INFORMATION

Additional supporting information can be found online in the Supporting Information section at the end of this article.

How to cite this article: Franke B, Schlief A, Walczak L, Sündermann S, Unbehaun A, Kempfert J, et al. Comparison of hemodynamics in biological surgical aortic valve replacement and transcatheter aortic valve implantation: An in-silico study. Artif. Organs. 2023;47:352–360. https://doi.org/10.1111/aor.14405